

9832-45765-2-PB.pdf

by Istyastono_11 Enade

Submission date: 30-Aug-2017 12:08PM (UTC+0700)

Submission ID: 841158731

File name: 9832-45765-2-PB.pdf (545.68K)

Word count: 4918

Character count: 23971

ELECTRONIC ABSORPTION SPECTRA OF SOME PHOTOSENSITIZERS BEARING CARBOXYLIC ACID GROUPS: INSIGHTS FROM THEORY

ASMIYENTI DJALIASRIN DJALIL^{1,2*}, ENADE PERDANA ISTYASTONO³, SLAMET IBRAHIM¹,
DARYONO HADI TJAHJONO¹

¹School of Pharmacy, Bandung Institute of Technology, Jalan Ganesha 10 Bandung 40132, Indonesia, ²The University of Muhammadiyah Purwokerto, Jl. Raya Dukuhwaluh, PO. Box 202 Purwokerto 53182, Indonesia, ³Laboratorium Teknologi Farmasi, Universitas Sanata Dharma, Yogyakarta, Indonesia
Email: asmiyenti@yahoo.com

Received: 08 Nov 2015 Revised and Accepted: 17 May 2016

ABSTRACT

Objective: The main objective of this research work was to give insight from theory in interpreting electronic absorption spectra of tetrapyrrolic macrocycles bearing carboxylic acid groups: protoporphyrin IX, pheophorbide *a* and its 1-hydroxyethyl derivatives for application in photodynamic therapy.

Methods: All calculations were carried out by using the Gaussian 03W version 6.0. Electronic excitation energies and oscillator strengths were computed as vertical excitations from the minima of the ground state structures by using ZINDO and TD-DFT approach in vacuo. The simulated spectra were obtained by using the GaussSum 2.2.0 program.

Results: The results showed that chlorine compounds (pheophorbide *a* and its 1-hydroxyethyl derivative) display the red-most absorption (Q_x) at longer wavelengths and their absorption were stronger than porphyrin compounds (protoporphyrin IX and its 1-hydroxyethyl derivative). On the other hand, the 1-hydroxyethyl derivatives were not able to red-shift the absorption compared to the parent compounds.

Conclusion: The chlorine compounds bearing carboxylic acid groups were, however, more promising candidates to be utilized in PDT compared to the corresponding porphyrin compounds.

Keywords: Absorption spectra, 1-Hydroxyethyl derivative, Photodynamic therapy, Pheophorbide *a*, Protoporphyrin IX, TD-DFT, ZINDO

© 2016 The Authors. Published by Innovare Academic Sciences Pvt Ltd. This is an open access article under the CC BY license (<http://creativecommons.org/licenses/by/4.0/>)

INTRODUCTION

PDT is a treatment technique for cancer and for certain benign conditions which utilizes a combination of visible light and a photosensitizer to produce reactive oxygen species in cells [1]. Photosensitizer is activated under irradiation, and the energy is then transferred to nearby molecules via a radiationless transition. In particular, triplet molecular oxygen (3O_2) is excited to the singlet state that is cytotoxic and can then destroy nearby cancer cells. In comparison to other currently available cancer therapeutic methods, PDT has the advantage of preferential accumulation of the photosensitizer in the tumor tissue and precise selectivity of the treatment by controlling the light [2].

The most widely used photosensitizer, photofrin (porfimer sodium), used mainly in the treatment of esophageal cancer and non-small cell lung cancer, illustrates the main problems of today's photosensitizers. Its red-most absorption maximum lies at a too short wavelength to achieve optimal tissue penetration, and the extinction coefficient for this absorption is low [3]. Photosensitizers with the red-most absorption at as long wavelength as possible and with enhanced absorption in this region are necessary for successful application of PDT.

We present here our work on some tetrapyrrolic macrocycles bearing carboxylic acid groups. In general, the 1-hydroxyethyl substituent increases the hydrophilicity of the compound, an advantage when the drug is administrated systemically. The 1-hydroxyethyl derivative of protoporphyrin IX (PPIX) was synthesized using addition reaction with hydrobromide, followed by nucleophilic substitution with H_2O [4]. We have found that the 1-hydroxyethyl derivative of PPIX efficiently generates singlet oxygen than those with parent compound when irradiated with visible light. Furthermore, the 1-hydroxyethyl derivative of PPIX showed lower dark toxicity in a normal cell compared to the parent compound [5]. In the continued effort to design, synthesize and characterize new

photosensitizers that exhibit a high-efficiency base on its absorption spectra, information from modern theoretical methods is very useful. In this paper, we show the absorption spectra prediction to assess the best molecules for PDT applications.

The most widely used method to calculate absorption spectra is a time-dependent density functional theory (TD-DFT) which, despite the fact that it is a single-reference method, has proven sufficiently accurate in many studies [6]. However, the performance of TD-DFT much depends on the actual functional used in the excited state calculations [7-9]. The studies show that the results can deviate significantly from experiments and that the performance of the functionals often is system specific. On the other hand, several prediction of UV-Vis spectra were performed using ZINDO [10-11]. In general, DFT methods (TD-DFT) had an extra calculation time cost compared to semiempirical methods (ZINDO). The theoretical works presented here were focused on the structural, energetic and spectroscopic behavior of protoporphyrin IX (1a), pheophorbide *a* (2a) and its 1-hydroxyethyl derivative (1b, 2b) (fig. 1). ZINDO and TD-DFT were used for this purpose. On the other hand, we take advantage of the λ_{max} at Q_x band predicted by these two methods in order to reach a better agreement between theoretical estimates and experimental measurements.

MATERIALS AND METHODS

All calculations were carried out using the Gaussian03W [12]. Geometry optimizations were performed by the density functional theory (DFT), B3LYP hybrid functional with 6-31G(d) basis set [13]. Structures were fully optimized in vacuo. No symmetry constraints were imposed during the geometry optimizations. Electronic excitation energies and oscillator strengths were computed as vertical excitations from the minima of the ground-state structures by ZINDO and TD-DFT approach in vacuo, respectively. The TD-DFT absorption spectra calculations were carried out using B3LYP with standard 6-31G(d) basis set [14]. The simulated spectra were

obtained using the GaussSum 2.2.0 program [15]. In comparing the theoretical and experimental data, we adjusted a fixed constant value (k) of a parent compound (**1a**, **2a**) to its 1-hydroxyethyl derivative.

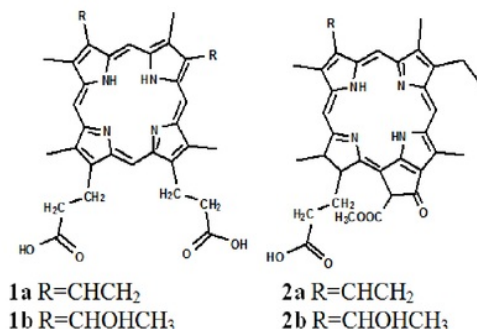


Fig. 1: Molecular structures of protoporphyrin IX (**1a**), pheophorbide *a* (**2a**) and its 1-hydroxyethyl derivatives

RESULTS AND DISCUSSION

Geometry optimization

The optimized configurations of all molecules are depicted in fig. 2. The optimized structure showed a planar geometry, which is comparable to those reported earlier [8, 16]. Total energy of **1a**, **1b**, **2a**, and **2b** were -1152102, -1248032, -1223981, and -1271943 kcal/mol, respectively. The 1-hydroxyethyl derivative of compounds studied has smaller total energy than the parent compounds.

Electronic absorption calculations in vacuo and comparison with experimental spectra

The experimental electronic spectra of porphyrins are very specific. Because of their highly conjugated ring, porphyrin-like systems show an intense band ($\epsilon \sim 200000$) at about 400 nm called the Soret or B band while in the region of 500-600 nm there are usually four weaker distinct of Q bands. Q bands have the low energy $S_0 \rightarrow S_1$ transitions (Q-bands) that are nearly forbidden by parity rules as a result of the high D_{2h} symmetry while B band has the most intense appears at higher energy allowed $S_0 \rightarrow S_2$ transition [17].

The spectroscopic behavior of tetra pyrrolic macrocycles can be rationalized in terms of the Gouterman four-orbital model, where the principal excitations involve the two highest occupied molecular orbitals (HOMO and next-HOMO) and the two lowest unoccupied orbitals (LUMO and next-LUMO) [17]. These energies are shown in fig. 3. The Gouterman's four level model of the compounds predicts that these four frontier orbitals are separated by a gap of 2.5 to 2.9 eV by ZINDO methods and 4.5 to 4.8 eV by TD-DFT (table 1). An HOMO-LUMO gap of chlorine (**2a**, **2b**) is lower than porphyrins (**1a**, **1b**). Furthermore, it can be seen that the Δ_{H-L} of **1a** and **1b** have nearly the same energy, as well as for **2a** and **2b**. The energy difference between HOMO and HOMO-1 orbitals as well as the LUMO and LUMO+1 orbitals for the porphyrin compounds (**1a**, **1b**) are small, in particular when the energies are calculated with ZINDO method.

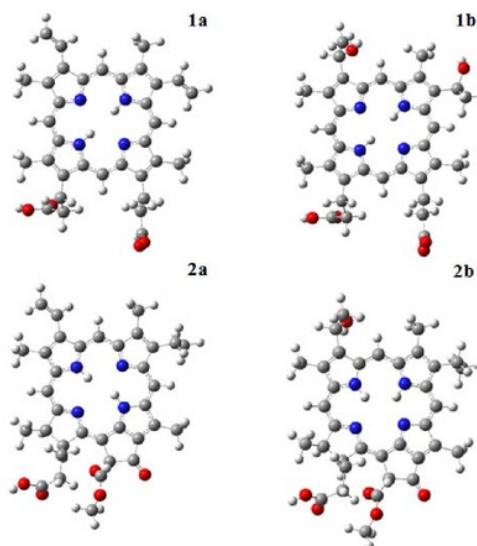


Fig. 2: Optimized geometry of **1a**, **1b**, **2a**, and **2b**

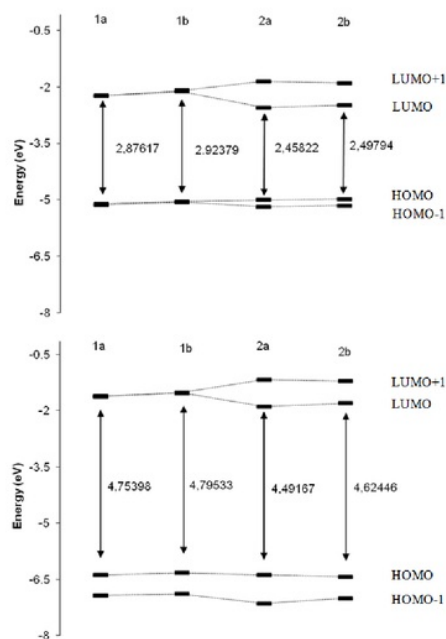


Fig. 3: Orbital energy levels for the four Gouterman orbitals of **1a**, **1b**, **2a**, and **2b** by ZINDO (top) and TD-DFT methods (bottom)

Table 1: Negative of the HOMO ($-E_{HOMO}$) and LUMO energies ($-E_{LUMO}$), and HOMO-LUMO gaps (Δ_{H-L}) calculated by ZINDO and TD-DFT in eV

| | TD-DFT | | | | ZINDO | | | |
|----------------|---------|---------|---------|---------|---------|---------|---------|---------|
| | 1a | 1b | 2a | 2b | 1a | 1b | 2a | 2b |
| $-E_{HOMO}$ | 6.38145 | 6.32784 | 6.38472 | 6.42662 | 5.11207 | 5.04922 | 5.00459 | 4.98309 |
| $-E_{LUMO}$ | 1.62747 | 1.53251 | 1.89303 | 1.80216 | 2.23590 | 2.12543 | 2.54637 | 2.48515 |
| Δ_{H-L} | 4.75398 | 4.79533 | 4.49167 | 4.62446 | 2.87617 | 2.92379 | 2.45822 | 2.49794 |

Electronic spectra of the compounds in the gas phase calculated by ZINDO and TD-DFT are shown in table 2 and table 3, respectively. The results show the main excitation energies, along with their relative oscillator strengths and the transition character. The optical band gap obtained from spectra is the lowest transition (or excitation) energy from the ground state to the first dipole-allowed excited state, which is an assumption that the lowest singlet excited state can be explained by only one single excited configuration, in which an electron is promoted from the HOMO to the LUMO. In fact, the optical band gap is not the orbital energy difference between the HOMO and LUMO, but the energy difference between the S_0 state and S_1 state. Only when the excitation to the S_1 state corresponds almost exclusively to the promotion of an electron from the HOMO to the LUMO, can the optical band gap be approximately equal to the HOMO-LUMO gap in quantity [18].

On the basis of the Gouterman four-orbital theoretical model, the Q_x -band is mainly due to two electronic transitions, named Q_x and Q_y .

The Q_x transition arises from the HOMO \rightarrow LUMO (in brief notation 0-0) electronic excitation with a contribution from the HOMO-1 \rightarrow LUMO+1 (1-1), whereas the Q_y transition is composed of the HOMO-1 \rightarrow LUMO (1-0) and HOMO \rightarrow LUMO+1 (0-1) electronic excitations [18,19]. Summarized in table 2 and table 3, the Q_x band (first excited state) is mainly composed of the HOMO \rightarrow LUMO transition (33 - 73%) with a smaller amount of the next-HOMO \rightarrow next-LUMO (16-43%). The next-HOMO \rightarrow next LUMO electronic excitation contributes in a higher amount by TD-DFT compared to ZINDO method. The Q_x transition corresponds to the strong experimental band that plays the basic role in PDT applications.

This can be assigned to a $\pi \rightarrow \pi^*$ transition. The Q_y band counterpart equally corresponds to next-HOMO \rightarrow LUMO and HOMO \rightarrow next-LUMO excitations. This second excitation energy falls between 1.82-2.04 eV with a weak intensity ($0.01 < f < 0.07$) by employing the ZINDO. Moreover TD-DFT calculated the energy falls between 2.27-2.39 eV with intensity ($0.01 < f < 0.04$).

Table 2: Excitation energies (eV and nm), oscillator strengths (f) and main configurations obtained by ZINDO. All electronic states belong to 1A

| Molecule | Excited state | Main configurations ^a | energy (eV) | λ (nm) | f |
|----------|---------------|---|-------------|----------------|--------|
| 1a | 1 | 34% (1-1)+60% (0-0) | 1.6191 | 765.75 | 0.06 |
| | 2 | 31% (1-0)+64% (0-1) | 1.8217 | 680.59 | 0.0712 |
| | 3 | 10% (3-1)+25% (2-1)+31% (1-1)+21% (0-0) | 3.0555 | 405.77 | 1.0973 |
| | 4 | 11% (3-1)+15% (2-1)+41% (1-0)+20% (0-1) | 3.2384 | 382.85 | 1.7136 |
| | 5 | 23% (3-1)+25% (2-1)+21% (1-0)+10% (0-1) | 3.2826 | 377.70 | 0.8268 |
| | 6 | 80% (0-2)+3% (3-1)+2% (2-0)+3% (1-6) | 3.4044 | 364.19 | 0.02 |
| | 7 | 36% (3-1)+12% (2-1)+25% (1-1)+11% (0-0) | 3.5645 | 347.83 | 1.6592 |
| | 8 | 85% (2-0)+5% (2-1) | 3.7294 | 332.45 | 0.1578 |
| | 9 | 38% (1-2)+23% (0-5)+19% (0-6)+7% (0-7) | 3.9034 | 317.63 | 0.0083 |
| | 10 | 86% (3-0) | 3.9469 | 314.13 | 0.1483 |
| 1b | 1 | 32% (1-1)+56% (0-0)+3% (1-0)+5% (0-1) | 1.6336 | 758.96 | 0.0549 |
| | 2 | 28% (1-0)+60% (0-1)+3% (1-1)+6% (0-0) | 1.8318 | 676.84 | 0.0752 |
| | 3 | 19% (3-1)+10% (2-1)+31% (1-1)+21% (0-0) | 3.1172 | 397.74 | 1.1955 |
| | 4 | 52% (1-0)+25% (0-1)+8% (1-1)+4% (0-0) | 3.3098 | 374.59 | 2.1125 |
| | 5 | 22% (3-1)+49% (2-1)+6% (3-2)+6% (2-0)+ | 3.3357 | 371.69 | 1.1483 |
| | 6 | 81% (0-2)+8% (1-5)+2% (0-3) | 3.4844 | 355.82 | 0.0033 |
| | 7 | 35% (3-1)+12% (2-1)+22% (1-1)+10% (0-0) | 3.6398 | 340.63 | 1.7086 |
| | 8 | 94% (10-4)+3% (3-4) | 3.8143 | 325.05 | 0.0011 |
| | 9 | 77% (2-0)+13% (2-1)+3% (2-5)+2% (0-2) | 3.8942 | 318.38 | 0.1254 |
| | 10 | 93% (11-3)+4% (11-2) | 3.9183 | 316.42 | 0.0004 |
| 2a | 1 | 16% (1-1)+72% (0-0)+3% (1-0)+4% (0-1) | 1.6068 | 771.62 | 0.2511 |
| | 2 | 36% (1-0)+52% (0-1)+7% (0-0) | 2.1303 | 582.00 | 0.0494 |
| | 3 | 38% (1-0)+31% (0-1)+11% (0-2)+6% (1-1) | 3.0107 | 411.81 | 1.7987 |
| | 4 | 14% (6-0)+43% (6-2)+11% (6-7)+9% (6-4) | 3.1259 | 396.63 | 0.0246 |
| | 5 | 13% (1-0)+33% (1-1)+19% (0-2)+9% (0-0) | 3.2378 | 382.92 | 1.2543 |
| | 6 | 34% (2-0)+23% (2-1)+23% (0-2) | 3.3876 | 365.99 | 0.2021 |
| | 7 | 31% (2-0)+24% (1-1)+31% (0-2)+5% (0-0) | 3.4673 | 357.58 | 0.537 |
| | 8 | 14% (3-0)+17% (2-0)+34% (2-1)+10% (1-2) | 3.7876 | 327.34 | 0.2786 |
| | 9 | 10% (4-0)+44% (3-0)+15% (1-2)+4% (7-0) | 3.8031 | 326.01 | 0.0437 |
| | 10 | 16% (2-1)+12% (1-2)+40% (0-5)+6% (2-0) | 3.8592 | 321.27 | 0.0339 |
| 2b | 1 | 21% (1-1)+73% (0-0) | 1.6585 | 747.56 | 0.1725 |
| | 2 | 46% (1-0)+48% (0-1) | 2.0447 | 606.36 | 0.0079 |
| | 3 | 39% (1-0)+40% (0-1)+8% (2-0) | 2.9607 | 418.76 | 1.4287 |
| | 4 | 19% (5-0)+32% (5-2)+7% (8-2)+7% (5-4) | 3.0161 | 411.07 | 0.0093 |
| | 5 | 56% (1-1)+19% (0-0)+8% (2-0)+5% (0-2) | 3.1842 | 389.37 | 1.4631 |
| | 6 | 48% (2-0)+15% (2-1)+13% (1-1) | 3.5273 | 351.50 | 0.7606 |
| | 7 | 63% (0-2)+13% (0-4)+5% (2-0) | 3.6958 | 335.47 | 0.2243 |
| | 8 | 42% (1-2)+11% (0-2)+20% (0-4)+3% (1-1) | 3.8621 | 321.03 | 0.3035 |
| | 9 | 36% (8-0)+17% (8-1)+18% (5-0)+10% (5-1) | 3.9083 | 317.23 | 0.0051 |
| | 10 | 96% (11-3) | 3.9197 | 316.31 | 0.0004 |

^aBy convention, in parentheses, the first number, n , is referred to as the occupied orbital contribution from HOMO- n , and the second, m , to the virtual one LUMO+ m .

The absorption spectra of the chlorins (2a, 2b) show striking differences from those of the porphyrins (1a, 1b). The Q_x band much more intense in the chlorins, and the lowest energy transition undergoes a bathochromic (red) shift. For example, TD-DFT calculated shows Q_x band ($\lambda = 579.96$ nm, $f = 0.1714$) for 2a compared with 1a ($\lambda = 563.95$ nm, $f = 0.005$). Chlorin compounds, in which one of the pyrrole double bonds has been saturated, are however more

promising candidates to be utilized in PDT as they display the red-most absorption (Q_x) at longer wavelengths and the absorption is stronger compared to the corresponding porphyrin compounds.

Fig. 4 and 5 indeed shows that Q_x band of chlorin compound (2b) at a longer wavelength becomes much more intense. In the chlorin, the component orbital energies of both the e_g (π^*) and the a_m (π) levels

become well separated (fig. 3). Although the energy of the lowest e_g (π^*) orbital does not increase much, that of the HOMO (a_{1u}) is successively raised. The overall result is that the energy of the

lowest transition (Q_x band) decrease along the sequence porphyrin-chlorin. At the same time, symmetry restrictions are removed or modified, and Q_x band becomes more intense.

Table 3: Excitation energies (eV and nm), oscillator strengths (f) and main configurations obtained by TD-DFT. All electronic states belong to 1A

| Molecule | Excited state | Main configurations | Energy (eV) | λ (nm) | f |
|----------|---------------|---|-------------|----------------|--------|
| 1a | 1 | 12% (1-0)+43%(1-1)+41% (0-0)+9% (0-1) | 2.1985 | 563.95 | 0.005 |
| | 2 | 38% (1-0)+12%(0-0)+41% (0-1)+9% (1-1) | 2.3476 | 528.13 | 0.0142 |
| | 3 | 48% (2-0)+20%(2-1)+6% (1-0)+7% (0-1) | 2.9298 | 423.18 | 0.1333 |
| | 4 | 16% (2-0)+64%(2-1)+4% (3-0)+3% (1-0) | 3.0430 | 407.44 | 0.048 |
| | 5 | 28% (3-0)+24%(3-1)+21% (2-0)+7% (0-1) | 3.1173 | 397.73 | 0.1916 |
| | 6 | 13% (3-0)+25% (3-1)+14% (1-1)+13% (0-0) | 3.2797 | 378.03 | 0.5096 |
| | 7 | 37% (3-0)+18% (3-1)+6% (4-1)+3% (1-0) | 3.4197 | 362.56 | 0.5941 |
| | 8 | 25% (3-1)+4% (4-0)+8% (3-0)+5% (2-0) | 3.5009 | 354.15 | 0.8779 |
| | 9 | 76% (4-0)+8% (4-1) | 3.6218 | 342.33 | 0.1557 |
| | 10 | 11% (4-0)+73% (4-1)+5% (0-2) | 3.6605 | 338.71 | 0.0865 |
| 1b | 1 | 20% (1-0)+29% (1-1)+33% (0-0)+24% (0-1) | 2.2367 | 554.31 | 0.0031 |
| | 2 | 30% (1-0)+22% (1-1)+20% (0-0)+27% (0-1) | 2.3870 | 519.41 | 0.0071 |
| | 3 | 21% (3-0)+19% (3-1)+14% (1-0)+11% (0-1) | 3.1405 | 394.79 | 0.3663 |
| | 4 | 46% (2-0)+43%(2-1)+2% (3-0) | 3.2330 | 383.49 | 0.0137 |
| | 5 | 19% (3-0)+17%(3-1)+12% (1-1)+13% (0-0) | 3.3494 | 370.17 | 0.4964 |
| | 6 | 43% (2-0)+45%(2-1)+3% (3-1) | 3.4061 | 364.00 | 0.0229 |
| | 7 | 30% (3-0)+25% (3-1)+3% (1-0)+9% (1-1) | 3.5617 | 348.10 | 0.7446 |
| | 8 | 21% (3-0)+28% (3-1)+8% (1-0)+9% (0-1) | 3.6791 | 336.99 | 1.0185 |
| | 9 | 64% (4-0)+23% (4-1)+2% (5-0)+3% (0-2) | 3.8895 | 318.76 | 0.0297 |
| | 10 | 19% (4-0)+56% (4-1)+16% (1-2) | 3.9873 | 310.95 | 0.0218 |
| 2a | 1 | 28% (1-1)+68% (0-0) | 2.1378 | 579.96 | 0.1714 |
| | 2 | 64% (1-0)+31%(0-1) | 2.3246 | 533.35 | 0.0277 |
| | 3 | 92% (2-0) | 2.9650 | 418.16 | 0.001 |
| | 4 | 16% (2-1)+42%(1-1)+6% (1-2)+6% (0-0)+7 | 3.1736 | 390.67 | 0.478 |
| | 5 | 11% (4-0)+35% (0-1)+4% (2-1)+9% (1-0) | 3.2396 | 382.71 | 0.6766 |
| | 6 | 77% (4-0)+6% (4-2)+4% (0-1) | 3.2854 | 377.38 | 0.0929 |
| | 7 | 90% (3-0) | 3.3595 | 369.05 | 0.0063 |
| | 8 | 63% (2-1)+10% (0-2)+7% (1-1)+7% (1-2) | 3.5807 | 346.25 | 0.3031 |
| | 9 | 73% (0-2)+2% (6-0)+4% (2-1)+2% (1-1) | 3.7257 | 332.78 | 0.1372 |
| | 10 | 13% (7-0)+59% (1-2)+3% (5-0)+3% (2-1) | 3.8259 | 324.06 | 0.4290 |
| 2b | 1 | 10% (1-0)+25% (1-1)+59% (0-0)+4% (0-1) | 2.1497 | 576.75 | 0.0929 |
| | 2 | 55% (1-0)+29%(0-1)+3% (1-1)+9% (0-0) | 2.2739 | 545.25 | 0.0447 |
| | 3 | 87% (3-0)+2% (3-1)+4% (3-2) | 3.0046 | 412.65 | 0.0056 |
| | 4 | 29% (2-0)+36% (0-1)+2% (3-0)+7% (1-0) | 3.0532 | 406.08 | 0.2833 |
| | 5 | 16% (2-0)+42% (1-1)+7% (1-2)+7% (0-0) | 3.2524 | 381.21 | 0.6066 |
| | 6 | 42% (2-0)+13%(1-1)+7% (0-1)+8% (0-2) | 3.3540 | 369.66 | 0.5987 |
| | 7 | 89% (5-0)+4% (7-0) | 3.5294 | 351.29 | 0.006 |
| | 8 | 94% (4-0) | 3.6721 | 337.64 | 0.045 |
| | 9 | 87% (6-0)+4% (2-1) | 3.8264 | 324.02 | 0.0077 |
| | 10 | 78% (3-1)+6% (5-1)+2% (3-0)+8% (2-1) | 3.8437 | 322.56 | 0.0032 |

^aBy convention, in parentheses, the first number, n , is referred to as the occupied orbital contribution from HOMO- n , and the second, m , to the virtual one LUMO+ m .

Gaussian 03 software was used to predict the electronic absorption spectra of compounds. One of the advantages of this software is that it includes a module to represent the curve of the spectrum (sum of Gaussian curves) calculated from the oscillator strengths and the wavelengths making easier to visualize the results. The simulated absorption spectrum was constructed using the oscillator strengths calculated at the ZINDO (fig. 4) and TD-DFT level of theory (fig. 5), fitted to a Gaussian distribution with a full-width at half-maximum (fwhm) of 3000 cm^{-1} .

Three or four intense transitions were observed in the B-band region. Two weak transitions are observed in the low-energy Q-band region of the calculated absorption spectrum (Q_x and Q_y band). A visual comparison between the Gaussian fits and the experimental spectra (fig. 6) indicates that the computed spectra pattern look remarkably similar to the experimental spectra without the vibronic overtones in the Q-band region.

The substitution of vinyl groups with 1-hydroxyethyl has little influence on the gap and thus on Q_x bands. ZINDO method shows that Q_x bands are slightly blue-shifted as one goes from 1a (765.75 nm) to 1b (758.96 nm), as well as from 2a (771.62 nm) to 2b

(747.56 nm). The same trend is observed by a TD-DFT method. They are slightly blue-shifted as one goes from 1a (563.95) to 1b (554.31 nm), as well as from 2a (579.96 nm) to 2b (576.75 nm).

These patterns are in good agreement with experimental data (table 4). In this work, although the absorption bands did not match exactly with experiment, the relative shifts in absorption as a function of 1-hydroxyethyl substitution were shown to correlate very well. These data are important and indicate that the computed values of all compounds studied should by analogy correlate with one another, and will be useful in predicting the absorption spectrum of the yet-to-be prepared other compounds.

A comparison of the ratios of the Soret band and Q-band extinction coefficients in the experimental spectra with the relative extinction coefficients in the computed spectra indicate that they are quite similar (table 4). The experimental spectra show a relative ratio of 100:4.5:3.4 for the Soret: Q_x : Q_y -band extinction coefficients in 1a. In the computed spectra, the analogous ratios of the extinction coefficients are 100:4.1:3.5 for 1a by ZINDO and 100:1.6:0.6 by TD-DFT method. With this information as a benchmark, we calculated the Soret: Q_x : Q_y -band relative ratio of the not-yet synthesized 2b.

Based on the ZINDO method, the Soret: Q_x : Q_y -band relative ratio of 2b is 100:5.4:11.8. Whereas, using TD-DFT method the Soret: Q_x : Q_y -band relative ratio of 2b is 100:6.4:13.3.

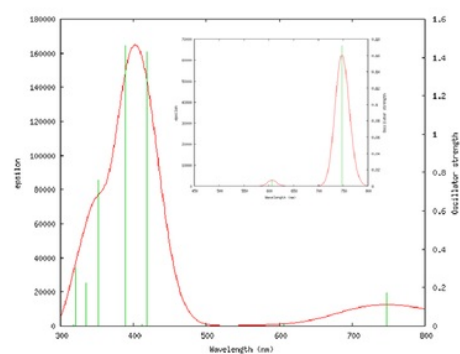
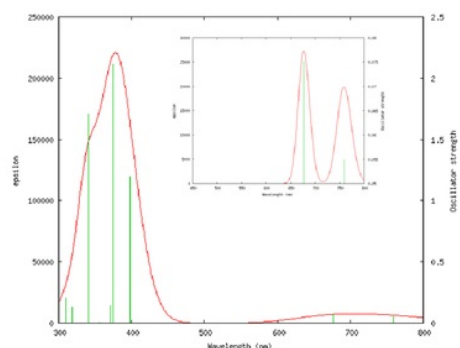


Fig. 4: Simulated electronic spectra for 1b (top) and 2b (bottom) by ZINDO fitted to a Gaussian distribution with fwhm of 3000 cm^{-1} . The inset in the upper right shows an expanded view of the Q-band region with fwhm 600 cm^{-1}

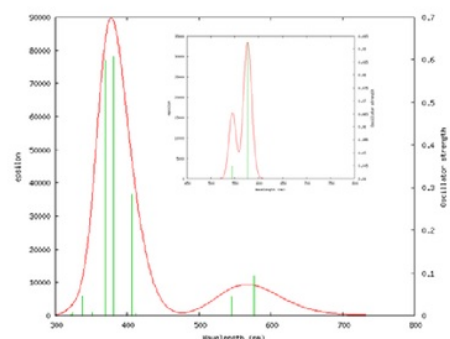
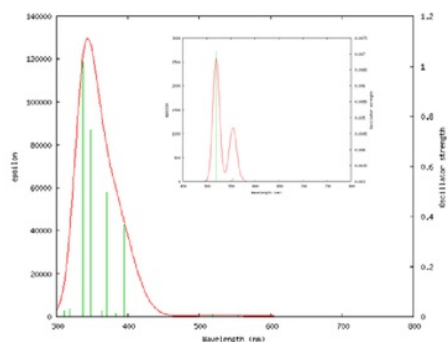


Fig. 5: Simulated electronic spectra for 1b (top) and 2b (bottom) by TD-DFT fitted to a Gaussian distribution with fwhm of 3000 cm^{-1} . The inset in the upper right shows an expanded view of the Q-band region with fwhm 600 cm^{-1}

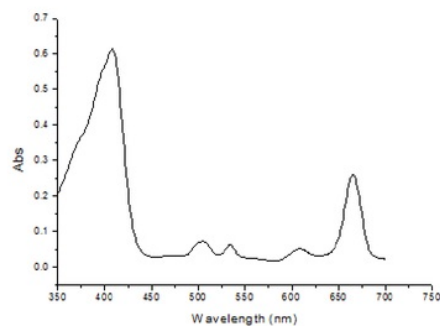
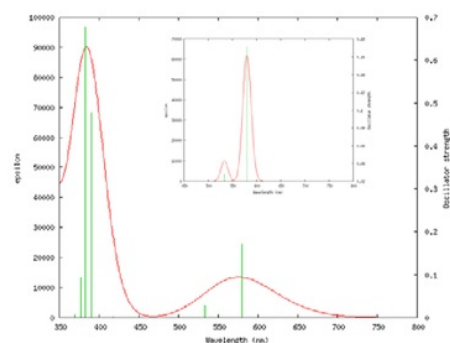


Fig. 6: Calculated (top) and experimental (bottom) spectra of pheophorbide a (2a)

Table 4: Relative ratio of observed extinction coefficient (ϵ) Q_x , Q_y , Soret band, and comparison with calculated results

| Compounds | λ_{cal} B, Q_y , Q_x (nm); ϵ soret: Q_y : Q_x ^a | λ_{cal} B, Q_y , Q_x (nm); ϵ soret: Q_y : Q_x ^b | λ_{obs} B, Q_y , Q_x (nm); ϵ soret: Q_y : Q_x ^c |
|-----------|---|---|---|
| 1a | 383, 681, 766; 100:4.1:3.5 | 361, 528, 563; 100:1.6:0.6 | 405, 576, 630 (in DMF); 100:4.5:3.4 |
| 1b | 378, 677, 759; 100:3.4:2.5 | 344, 519, 554; 100:0.6:0.3 | 402, 572, 625 (in methanol); 100:4.8:2.7 |
| 2a | 399, 582, 772; 100:3.0:15.5 | 385, 533, 579; 100:4.4:27.1 | 408, 609, 665 (in diethylether); 100:7.2:46.0 |
| 2b | 402, 606, 747; 100:5.4:11.8 | 378, 545, 577; 100:6.4:13.3 | |

^aElectronic absorption calculations by ZINDO, ^belectronic absorption calculations by TD-DFT, ^celectronic absorption experimental.

Table 5: Observed Q_x band and corresponding Q_x band calculated results

| Compounds | λ_{obs} (nm) ^a | λ_{cal} (nm) ^b | | λ_{cal} (nm) ^c | |
|-----------|--|--|--------|--|--------|
| | | ZINDO | TD-DFT | ZINDO | TD-DFT |
| 1a | 630 (in DMF) | 766 | 564 | 630 | 630 |
| 1b | 625 (in methanol) | 759 | 554 | 624 | 619 |
| 2a | 665 (in diethyl ether) | 772 | 580 | 665 | 665 |
| 2b | | 747 | 577 | 643 | 662 |

^a: The observed band; ^b: Calculated Q band based on ZINDO and TD-DFT; ^c: Calculated Q band based on ZINDO and TD-DFT with adjusted *k* value: ZINDO results multiply by 0.822 (for porphyrin), 0.861 (for chlorin); TD-DFT results multiply by 1.117 (for porphyrin), 1.147 (for chlorin).

One can also note that the Q band excitation energy by ZINDO method tend to overestimate. The different trend was observed for B bands: we calculated them to be at 383 nm and 378 nm for 1a and 1b, respectively, whereas experiments report respective values of 405 and 402 nm. These bands are nonetheless not implied in phototherapy processes, so we do not analyze here in this part of the spectrum. The Q band excitation energy estimation by TD-DFT tend to be low compared with the experimental data. These results differ from those reported by Palma *et al.* [8]. The differences of estimation and experiment data for TD-DFT and ZINDO method were 87-90% dan 78-84%, respectively. Considering the differences values reveal the TD-DFT more accurately than ZINDO method.

Liu *et al.* [21] and Yuan *et al.* [22] reported that the visible absorption maxima can be precisely calculated by ZINDO/S method by adjusting OWF π - π value (the relationship between π - π overlap weighting factor) OWF π - π . In this work, although the absorption bands did not match exactly with experiment, we tried to correlate with the experimental results. After conversion with adjusted *k* value, the predicted absorption maxima of 2b are 643 nm by ZINDO method and 662 nm by the TD-DFT method (table 5).

CONCLUSION

Electronic absorption spectra of PPIX, pheophorbide *a* and its 1-hydroxyethyl derivatives were predicted within ZINDO and TD-DFT methods. The spectra were analyzed and compared with available experimental data. The chlorin compounds bearing carboxylic acid groups were, however, more promising candidates to be utilized in PDT compared to the corresponding porphyrin compounds. Although the absorption bands did not match exactly with experiment, the relative shifts and intensity as a function of a 1-hydroxyethyl substitution and reduction of pyrrole ring were shown to correlate very well. Overall, the prediction by using TD-DFT reveal more accurately than ZINDO approach.

CONFLICT OF INTERESTS

Declared none

REFERENCES

- Castano AP, Demidova TN, Hamblin MR. The mechanism in photodynamic therapy: part one-photosensitizers, photochemistry and cellular localization. *Photodiagn Photodyn Ther* 2004;1:279-93.
- Maiya BG. Photodynamic therapy: 2. Old and new photosensitizers. *Resonance* 2000;15-29.
- Ormond AB, Freeman HS. Dye sensitizers for photodynamic therapy. *Materials* 2013;6:817-40.
- Mwakwari SC. Syntheses and properties of iso porphyrins and related derivatives for application in photodynamic therapy [dissertation]. Louisiana (United States): Louisiana State University and Agricultural and Mechanical College; 2007.
- Djalil AD, Nurulita NA, Limantara L, Ibrahim S, Tjahjono DH. Biological evaluations of protoporphyrin IX, pheophorbide *a*, and its 1-hydroxyethyl derivatives for application in photodynamic therapy. *Int J Pharm Pharm Sci* 2012;4:741-6.
- Eriksson ESE, Eriksson LA. Computational design of chlorin-based photosensitizers with enhanced absorption properties. *Phys Chem Chem Phys* 2011;13:11590-6.
- Perpete EA, Wathelot V, Preat J, Lambert C, Jacquemin D. Toward a theoretical quantitative estimation of the λ_{max} of anthraquinones-based dyes. *J Chem Theory Comput* 2006;2:434-40.
- Palma M, Cardenas-jiron GI, Rodriguez MIM. Effect of chlorin structure on theoretical electronic absorption spectra and on the energy released by porphyrin-based photosensitizers. *J Phys Chem A* 2008;112:13574-83.
- Tian BX, Eriksson ESE, Eriksson LA. Can range-separated and hybrid DFT functionals predict low-lying excitations? A tookad case study. *J Chem Theory* 2010;6:2086-94.
- Khan MS, Khan ZH. Ab initio and semiempirical study of the structure and electronic spectra of a hydroxyl substituted naphthoquinones. *Spectrochim Acta Part A* 2005;61:777-90.
- Eshimbetov AG, Kristallovich EL, Abdullaev ND, Tulyaganov TS, Shakhidoyatov KhM. AM1/CI, CNDO/S and ZINDO/S computations of absorption bands and their intensities in the UV spectra of some 4(3H)-quinazolinones. *Spectrochim Acta Part A* 2006;65:299-307.
- Frisch MJ, Trucks GW, Schlegel HB, Scuseria GE, Robb MA, Cheeseman JR, *et al.* Gaussian 03 revision B.04. Wallingford CT: Gaussian, Inc; 2004.
- Francl MM, Petro WJ, Hehre WJ, Binkley JS, Gordon MS, DeFrees DJ, *et al.* Self-consistent molecular orbital methods. XXIII. A polarization type basis set for second-row elements. *J Chem Phys* 1982;77:3654-65.
- Liu YL, Feng JK, Ren AM. Structural, electronic, and optical properties of phosphole-containing p-conjugated oligomers for light-emitting diodes. *J Comput Chem* 2007;28:2500-9.
- O'Boyle NM, Vos JG. GaussSum 1.0. Dublin, Ireland: Dublin City University; 2005. Available from: <http://gausssum.sourceforge.net>. [Last accessed on 10 Oct 2015].
- Ghosh A. A comparative theoretical study of free-base porphyrin, chlorin, bacteriochlorin, and isobacteriochlorin: evaluation of the potential roles of ab initio hartree-fock and density functional theories in hydroporphyrin chemistry. *J Phys Chem B* 1997;101:3290-7.
- Gouterman M, Wagniere GH, Snyder LC. Spectra of porphyrins: Part II. Four orbital model. *J Mol Spectrosc* 1963;11:108-27.
- Quartarolo AD, Russo N, Sicilia E, Lelj F. Absorption spectra of the potential photodynamic therapy photosensitizers texaphyrins complexes: a theoretical analysis. *J Chem Theory Comput* 2007;3:860-9.
- Petit L, Quartarolo A, Adamo C, Russo N. Spectroscopic properties of porphyrin-like photosensitizers: insights from theory. *J Phys Chem B* 2006;110:2398-404.
- Liu JN, Chen ZR, Yuan SF. Study on the prediction of visible absorption maxima of azobenzene compounds. *J Zhejiang Univ Sci B* 2005;6:584-9.
- Yuan SF, Chen ZR, Cai HX. Calculation of visible absorption maxima of phthalocyanine compounds by quantum theory. *Chin Chem Lett* 2003;14:1189-92.

ORIGINALITY REPORT

0%

SIMILARITY INDEX

0%

INTERNET SOURCES

0%

PUBLICATIONS

0%

STUDENT PAPERS

PRIMARY SOURCES

Exclude quotes On

Exclude bibliography On

Exclude matches < 25%